Development of thymic tumor in [LSL:KrasG12D;Pdx1-CRE] mice, an adverse effect associated with accelerated pancreatic carcinogenesis

Sophie Liot
Laboratoire de Biologie Tissulaire et Ingénierie Thérapeutique (LBTI), UMR CNRS 5305, Université Claude Bernard Lyon 1, Institut de Biologie et Chimie des Protéines, 69367 Lyon Cedex 07, France

Naïma El Kholti
Laboratoire de Biologie Tissulaire et Ingénierie Thérapeutique (LBTI), UMR CNRS 5305, Université Claude Bernard Lyon 1, Institut de Biologie et Chimie des Protéines, 69367 Lyon Cedex 07, France

Bernard Verrier
Laboratoire de Biologie Tissulaire et Ingénierie Thérapeutique (LBTI), UMR CNRS 5305, Université Claude Bernard Lyon 1, Institut de Biologie et Chimie des Protéines, 69367 Lyon Cedex 07, France

Ulrich Valcourt
Laboratoire de Biologie Tissulaire et Ingénierie Thérapeutique (LBTI), UMR CNRS 5305, Université Claude Bernard Lyon 1, Institut de Biologie et Chimie des Protéines, 69367 Lyon Cedex 07, France

Elise Lambert (elise.lambert@ibcp.fr)
Laboratoire de Biologie Tissulaire et Ingénierie Thérapeutique (LBTI), UMR CNRS 5305, Université Claude Bernard Lyon 1, Institut de Biologie et Chimie des Protéines, 69367 Lyon Cedex 07, France

Research Article

Keywords: Pancreatic Ductal AdenoCarcinoma, KC mouse model, Thymic mass, KrasG12D expression

Posted Date: April 7th, 2021

DOI: https://doi.org/10.21203/rs.3.rs-383266/v1

Version of Record: A version of this preprint was published at Scientific Reports on July 23rd, 2021. See the published version at https://doi.org/10.1038/s41598-021-94566-x.

Development of thymic tumor in [*LSL:Kras^{G12D}*; *Pdx1-CRE*] mice, an adverse effect associated with accelerated pancreatic carcinogenesis

Short title: Thymic tumor development in KC mouse model is associated with accelerated pancreatic carcinogenesis.

Sophie LIOT[1], Naïma EL KHOLTI[1], Bernard VERRIER[1], Ulrich VALCOURT[1] and Elise LAMBERT[1,*]

[1] Laboratoire de Biologie Tissulaire et Ingénierie Thérapeutique (LBTI), UMR CNRS 5305, Université Claude Bernard Lyon 1, Institut de Biologie et Chimie des Protéines, 7, passage du Vercors, F-69367 Lyon Cedex 07, France.
* Correspondence should be addressed to E.L. (elise.lambert@ibcp.fr)

Abstract
Pancreatic Ductal AdenoCarcinoma (PDAC) represents about 90% of pancreatic cancers. It is one of the most aggressive cancer, with a 5-year survival rate below 10% due to late diagnosis and poor therapeutic efficiency. This bad prognosis thus encourages intense research in order to better understand PDAC pathogenesis and molecular basis leading to the development of innovative therapeutic strategies. This research frequently involves the KC (LSL:*Kras^{G12D}*;*Pdx1*-CRE) genetically engineered mouse model, which leads to pancreatic cancer predisposition. However, as frequently encountered in animal models, the KC mouse model also exhibits biases. Herein, we report a new adverse effect of *Kras^{G12D}* mutation in KC mouse model. In our hands, 10% of KC mice developed clinical signs reaching pre-defined end-points between 100- and 150-days post-parturition, and associated with large thymic mass development. Histological and genetic analyses of this massive thymus enabled us (1) to characterize it as a highly proliferative thymic lymphoma and (2) to detect the unexpected recombination of the Lox-STOP-Lox cassette upstream *Kras^{G12D}* allele and subsequent KRAS^{G12D} protein expression in all cells composing thymic masses. Finally, we highlighted that development of such thymic tumor was associated with accelerated pancreatic carcinogenesis, immune compartment disorganization, and in some cases, lung malignancies.

Keywords : Pancreatic Ductal AdenoCarcinoma, KC mouse model, Thymic mass, *Kras^{G12D}* expression

Introduction

Pancreatic cancer, among which Pancreatic Ductal AdenoCarcinoma (PDAC) represents about 90% of cases, is currently the seventh cause of cancer-related deaths worldwide, and is predicted to become second in industrialized countries over the next decade if no progress is made[1–3]. PDAC is one of the most aggressive cancer, with a 5-year survival rate below 10%, due to late diagnosis and poor therapeutic efficiency[4]. Indeed, PDAC develops without specific symptoms, leading to diagnosis at locally advanced or metastatic tumor stage[5,6]. As a consequence, only 20% of PDAC are resectable, and classical chemotherapies are inefficient, only prolonging patient lifespan by a few months[7]. Thus, PDAC is currently the subject of intense research to develop innovative therapeutic strategies, based on the understanding of PDAC pathogenesis and molecular basis.

Fundamental research in the field of oncology is based on the use of models recapitulating human pathology. In the case of PDAC, a large spectrum of models is available, including, from the farthest to the closest of human pathogenesis, 2D and 3D (organotypics) *in vitro* cell culture systems with tumor cell lines, organoids and animal models[8,9]. These latter are now widely used and comprise several experimental strategies. Historically, PDAC was chemically induced by the injection of potent carcinogens such as DMBA (7,12-DiMethylBenz(a)Anthracene) in the pancreas. This method has been abandoned in favor of xenografts (of tissues or cell lines derived from patients) and genetically-engineered mouse models (GEMM)[10,11], which can be considered to recapitulate as close as possible the carcinogenesis, invasive tumor progression and metastasis formation of PDAC. GEMM notably allow to study risk factors, genetic alterations, as well as PDAC initiation and progression, and represent a pre-clinical study platform for the development of new diagnosis methods and treatments[12–15].

First GEMM used in PDAC research were established by the overexpression of TGFα under the control of *Elastase* promoter (specific of pancreatic acinar cells)[16,17]. However, this model did not allow to trigger invasive PDAC and was then replaced by several models involving mutated *Kras* oncogene. KRAS (for Kristen RAS) is a small GTPase of the RAS family having a preponderant role in malignancies, since it is involved in several signaling pathways leading to the activation of cell proliferation[18–20]. Single KRAS amino-acid mutation, often on residue G12, results in KRAS constitutive activation and subsequent cell behavior modification. *KRAS* proto-oncogene mutations have been detected in about 30% of human tumors[21], and 92% of PDAC, where they correlate with a worse prognosis[22]. In PDAC, *KRAS* mutation is even considered as the first hit mutation (detected from the pre-malignant stages), leading to cell sensitivity to malignant transformation induced by the accumulation of other mutations (notably the inactivation of tumor suppressor genes *TP53*, *CDKN2A* (also named *INK4A*) and *SMAD4*) and chromosomal aberrations.

As a consequence, *Kras* mutation in mouse results in the development of malignancies[23]. In 2001, Jackson and colleagues developed a mouse model allowing to induce conditional KRAS activation thanks to the CRE-Lox system, with the mutated *Kras*^{G12D} oncogene placed downstream a Lox-STOP-Lox sequence (transcriptional STOP)[24]. This construct has then been used in 2003 in the same laboratory to create a pancreatic cancer predisposition model, in which the CRE recombinase expression is under the control of pancreas-specific gene promoters: *Pdx1* or *Ptf1a* (*p48*), allowing a tissue-specific expression of *Kras*^{G12D} (model named "KC", for [LSL:*Kras*^{G12D}*;Pdx1* or *Ptf1a*-CRE])[25]. These mice develop pancreatic preneoplastic lesions similar to human ones, but rarely evolving into PDAC. In order to counteract this long latency limiting PDAC progression study, other GEMM have been established with additional mutations in the [LSL:*Kras*^{G12D}*;Pdx1*-CRE] context, including *p53* ("KPC

model")[26] and *Ink4a* ("KIC model")[27] mutated tumor suppressor genes, enabling the development of invasive PDAC within few months[28].

Nowadays, KC mouse model (which will refer to [LSL:*Kras*^{G12D};*Pdx1*-CRE] from now) continues to be widely used, as it allows a good understanding of pancreatic pre-neoplastic lesions preceding invasive PDAC. Indeed, this model recapitulates the main characteristics of human pancreatic carcinogenesis, including desmoplastic reaction and PanIN linear development. It thus provides a better understanding of the key signaling pathways involved in these processes and is a suitable model for the search of an early diagnostic method[14]. However, it is still important to keep in mind that GEMM do not totally recapitulate human pathogenesis and may have some undesirable effects, and as such, experimental limitations and biases have been reported for the KC model. Indeed, Pdx1 (Pancreatic and duodenal homeobox 1) is a transcription factor activating the expression of various pancreatic proteins, such as insulin, and is highly involved in pancreas development, as this developmental factor is responsible for pancreatic identity induction[29,30]. As a consequence, KC model is a "pre-natal" model, in which *Kras*^{G12D} mutated oncogene will be expressed during early steps of pancreatic development, and thus does not exactly mimic the human pathogenesis[28,31,32]. Furthermore, at adulthood, *Pdx1* is classically expressed in duodenum and pancreas. In this latter, it has mainly been detected in nuclei of β cells (endocrine cells of Langerhans islets) and to a lesser extent in the nuclei of ductal and acinar cells[33,34]. Therefore, it is not possible to decipher the cells that are at the origin of PDAC using this model, since *Kras*^{G12D} will be expressed in the different pancreatic epithelial cells. Additionally, islet disorganization as well as lesions within the endocrine part of the pancreas have also been highlighted[35,36], showing some limitations of this model.

Herein, we reported a new adverse effect of *Kras*^{G12D} mutation in the KC mouse model, which has not yet been described. In our hands, between 100 and 150 days post-parturition, 10% of the KC mice developed clinical signs corresponding to pre-defined humane end-points, including weight loss and respiratory distress. At necropsy, all concerned mice presented a large thymic mass filling the entire space inside the rib cage, crushing the lungs, heart and esophagus. Histologically, we suggest that this thymic mass may correspond to a highly proliferative thymic lymphoma. In all concerned thymus, we detected the recombination of the Lox-STOP-Lox cassette upstream *Kras*^{G12D} allele and subsequent KRAS^{G12D} protein expression in all thymic mass cells, as opposed to normal thymus. In addition, we highlighted that development of such a thymic tumor was associated with accelerated pancreatic carcinogenesis and immune compartment disorganization (visible in the spleen), and observed some mice with lung malignancies. Our study thus alerts about the presence of a non-silent side effect of *Kras*^{G12D} mutation in 10% of KC mice, which may be missed if dissection is restricted to the abdominal cavity.

Results

In KC mouse model, LSL recombination occurs in pancreas but not in tail

KC mouse model were obtained by crossing the *Pdx1*-CRE and LSL:*Kras*^{G12D} mouse strains, in order to study pancreatic carcinogenesis. In the LSL:*Kras*^{G12D} strain, the endogenous *Kras*^{G12D} allele is preceded by a Lox-STOP-Lox (LSL) cassette avoiding *Kras*^{G12D} transcription in absence of recombination. In order to induce a conditional expression of the mutated oncogene in the pancreas, we used the *Pdx1*-CRE mouse strain, in which the CRE recombinase coding sequence is placed downstream of the *Pdx1* gene promoter (Figure 1A).

Mice were genotyped one-week post-parturition by a classic Polymerase Chain Reaction (PCR). All KC mice carried both the wild-type (WT) and the mutated (LSL:*Kras*^{G12D}) *Kras* alleles, while WT mice presented only the WT *Kras* band (Figure 1B, bottom). In order to confirm correct pancreas-specific recombination, conditional *Kras*^{G12D} PCR was performed on tail and pancreas of one KC mouse (Figure 1B, top). Primers used for this PCR, which allows to detect LSL cassette recombination, are presented on Figure 1A. In tail of KC mice, we observed wild-type (WT) and LSL:*Kras*^{G12D} bands only, while in pancreas we noted the presence of a third band (corresponding to *Kras*^{G12D} without the LSL cassette). The coexistence of the 3 bands in pancreas suggests that recombination is partial, not in all cells composing the tissue extract. As controls, we analyzed pancreatic DNA from (1) WT mouse pancreas, for which we detected the WT *Kras* allele only, with a large band, and (2) KC mouse tumor tissue with almost total recombination (CTRL+), which showed mainly the presence of the WT and *Kras*^{G12D} alleles without the LSL cassette. This result confirmed the correct pancreas-specific recombination of mutated *Kras*^{G12D} oncogene.

10% of KC mice display severe clinical signs associated with thymic mass development.

While constituting a KC cohort, we observed some mice suffering of severe clinical signs between 100- and 150-days post-parturition. These latter included weight loss (up to 4 grams in one week, Figure 2A) and respiratory distress, and corresponded to pre-defined end-points, thus leading us to euthanize the animals before the scheduled date (Figure 2B). These mice finally accounted for about 10% of the total cohort (9/89), which thus cannot be ignored. Here, we show 4 KC mice harboring such suffering signs in our cohort that we compare to 4 age-matched mice (100 and 150 days) without apparent symptoms from the same cohort. During dissection, we observed that all mice that reached a humane end-point had a rib cage invaded by a huge mass clearly developed from thymus. This thymic mass caused the crushing of esophagus, heart and lung, explaining the observed clinical signs (Figure 2C). It has to be noted that on the Figure 2C, lung and heart were clearly visible in the mouse with a histologically normal thymus (left photo), but completely hidden by the thymic mass in the symptomatic mouse (right photo).

Thymic masses are lymphocyte-rich and exhibit total LSL cassette recombination with subsequent KRAS^{G12D} expression.

We then performed histological analysis of these thymic masses and compared them to normal thymus. After paraffin-embedding, tissues were cut and sections were stained with Hematoxylin-Eosin or labelled by immunohistochemistry (IHC) for Ki67 (proliferation) (Figure 3A). As expected, normal thymus was composed of (1) a connective tissue capsule, (2) the cortex, which is darker and contains lymphocytes, some epithelial reticular cells and macrophages and (3) the medulla, containing larger lymphocytes and Hassall's Corpuscles. In contrast, the thymic masses did not show such organization, and seemed to be very rich in lymphocytes (round cells predominantly occupied by the nucleus), reminiscent of a thymic lymphoma. These cells were highly proliferative, as shown by the Ki67 immunolabelling.

Conditional *Kras*^{G12D} PCR were also performed on these tissues, in order to determine if LSL cassette recombination occurred, leading to *Kras*^{G12D} expression and the subsequent tumor development in the thymus (Figure 3B). Interestingly, we highlighted that normal thymus did not present any LSL cassette recombination, while the recombination was total in thymic masses. Indeed, in those tissues, we were not able to detect any LSL:*Kras*^{G12D} band, suggesting that all cells proceeded to LSL cassette recombination and thus expressed *Kras*^{G12D} allele. Moreover, such recombination seemed to be specific to the thymus, as no recombination of the LSL cassette was detected in the tail of mice

suffering from thymic mass development. It has to be noted that WT *Kras* amplicon was always visible in normal thymus, while it was sometimes difficult to discriminate in thymic masses. Thus, genotyping PCR was performed on tails from the same animals to confirm the heterozygosity of the $Kras^{G12D}$ allele for all KC mice (homozygous $Kras^{G12D/G12D}$ is lethal). Finally, the consequence of the LSL cassette excision was confirmed by performing an anti-$KRAS^{G12D}$ immunohistochemistry showing that all cells expressed $KRAS^{G12D}$ in thymic mass, while none were positive in normal thymus (Figure 3C). Therefore, it appeared that LSL cassette recombination and subsequent mutated $Kras^{G12D}$ oncogene expression occurred in thymus of 10% of KC mice, leading to the development of thymic mass (lymphoma-like tumor).

Thymic mass development is associated with accelerated pancreatic carcinogenesis, immune disorder and lung malignancies

Finally, we wanted to decipher if such thymic tumor development could have an effect on pancreatic carcinogenesis. We thus analyzed the pancreas of mice exhibiting or not a thymic mass, by classical H&E staining and Ki67, CK19 and $KRAS^{G12D}$ immunolabelling. We clearly noticed that mice with thymic tumor exhibited an accelerated pancreatic carcinogenesis, as they displayed larger area occupied by pre-tumoral lesions, and more advanced lesions in three of the four mice (Figure 4A, left). One of the mice also showed high level of infiltration, probably of immune cells, which were highly proliferative, and accompanied by the presence of large lymph nodes on section (Supplementary Figure S1).

We detected $KRAS^{G12D}$ mutated protein within preneoplastic lesions, as well as in Langerhans islets of all KC mouse pancreas, in contrast with WT mouse, which did not display any labelling. In addition, $KRAS^{G12D}$ was detected in acinar cells bordering pre-tumoral lesions, and that seemed to undergo Acinar-to-Ductal Metaplasia (ADM) (Figure 4A, right). We also observed some $KRAS^{G12D}$-positive cells in the spleen adjacent to pre-tumoral pancreatic lesions in KC mice with a thymic mass, suggesting proximal invasion in regard to cell and nucleus morphologies (Supplementary Figure S2).

Thymus being one of the primary lymphoid organs, we also investigated the immune compartment, notably thanks to spleen analysis. Interestingly, mice with thymic tumor displayed highly enlarge spleen, which seemed to be histologically disorganized (Figures 4B and 4C). Indeed, white pulp seemed larger, and less organized and dense, as it can be observed following H&E staining and Ki67 immunolabelling. In addition, $KRAS^{G12D}$ protein was detected in white pulp of spleen from mice developing thymic mass, suggesting either the recruitment of lymphocytes from the thymus or recombination of the LSL cassette within the spleen too. Interestingly, in the mouse with high level of immune infiltration, lymph nodes and immune cells present around pre-malignant cells were also $KRAS^{G12D}$ positive (Supplementary Figure S1).

Finally, in three out of four mice exhibiting thymic mass development, we also noticed proliferative (Ki67-positive) masses in lungs, positive for $KRAS^{G12D}$ (Figure 4D). These lung malignancies were negative for CK19 and did not show PDAC morphology. In one of them, such masses were even visible macroscopically at necropsy (Figure 4E).

In conclusion, mice developing thymic tumor seemed to have an accelerated pancreatic carcinogenesis and lung damages, potentially associated with immune perturbations.

Discussion

Taken together, our results highlight a new adverse effect linked to genetic modification in the KC mouse model. Indeed, we pointed out the development of thymic tumor in 10% of the KC mouse cohort, which cannot be ignored. Interestingly, our observations were made in two different animal facilities, indicating that it would better rely on intrinsic mechanism than on environmental cues. Mice presenting thymic mass reached humane end-points between 100 and 150 days post-parturition, including rapid weight loss and respiratory distress, probably due to lung, heart and esophagus crushing under the tumor mass, since these organs were smaller than in normal KC mice. In addition, those mice were prostrated in their cage, suggesting abdominal pain. Such symptoms are close to the ones developed in consequence to PDAC development and are thus confounding for this mouse model at early age. It must be noted that presence of this thymic mass could not be predict without opening rib cage, showing the importance to proceed to a complete necropsy.

Histologically, thymic masses showed a disorganized structure, with the absence of distinguishable cortex and medulla, in contrast to normal thymus. Tumors appeared to be lymphocyte-rich and highly proliferative, evoking thymic lymphoma, with few epithelial cells[37–39]. This diagnosis is further reinforced by the strong similarities observed at the macroscopic and microscopic levels between the pathological thymus of KC mice and the thymic lymphoma developed in the p53 KO mice[40].
We then investigated *Kras*^{G12D} expression within these thymic masses. To do so, we first analyzed LSL cassette recombination upstream *Kras*^{G12D} allele, and showed that the transcriptional STOP was deleted in all thymic masses, while it was never the case in normal thymus. Interestingly, this recombination was total, with no remaining allele with the LSL cassette, suggesting that all cells would have recombined, in contrast to pancreas where the LSL sequence persisted. This was confirmed by anti-KRAS^{G12D} immunohistochemistry, as we detected labelling in all cells from thymic masses, and not in normal thymus. Thus, we can confidently hypothesize that the development of such thymic tumors, would rely on the expression of mutated KRAS oncogene.

Initially, our hypothesis for such atypical *Kras*^{G12D} expression was that *Pdx1* could be expressed by thymic antigen-presenting cells for lymphocyte education, with subsequent *Kras*^{G12D} expression which could lead to malignant transformation in some cases (due to transient *Pdx1* expression). However, the described observations suggest another mechanism. The lymphoma-like phenotype of thymic tumoral mass, as well as the expression of *Kras*^{G12D} in all thymic cells (including lymphocytes) suggested that recombination could occur independently from *Pdx1* expression. Indeed, in the original study using *Kras*^{G12D} oncogene in mouse model, Johnson and colleagues studied the organs, which were sensitive to sporadic recombination (unequal sister chromatid exchange or intra-chromosomal recombination) leading to *Kras*^{G12D} expression. Interestingly, they highlighted the development of lung tumors, thymic lymphomas and papillomas, suggesting that lung, thymus and skin were the organs in which sporadic recombination occurred[41]. The development of thymic masses we observed could thus be relied on sporadic recombination. In addition, we frequently observed papillomas on KC mice, with no deleterious effect on animal well-being (data not shown), coherently with the study of Johnson and collaborators. We also highlighted that three of the four mice developing thymic mass exhibited some malignancies in lung, more or less visible, that were positive for KRAS^{G12D} and highly proliferative, as expected in consequence to KRAS activation. The mouse showing no lung disorder was dissected as scheduled, at 100 days, and had not reached humane end-points, suggesting that lung mass development could arise later. We thus observed here the same symptoms pointed out by Johnson and colleagues in 2001[41], which could be explained by sporadic recombination. This is encouraged by the fact that no correlation existed between pancreatic lesion extent and level of lung damage.

Moreover, lung malignancies were negative for CK19 and did not displayed PDAC morphology, thus ruling out the hypothesis of pancreatic metastasis, since lung is a known metastasis site for pancreatic tumor cells.
Therefore, we suggest here that *Pdx1*-CRE construct is not sufficient to restrain *Kras*^{G12D} recombination to the pancreas, and that sporadic recombination occurs in thymus (in 10% of cases), skin and lung. This is coherent with the fact that no evidence of *Pdx1* expression in the thymus has been found, and some articles even reported the absence of Pdx1 in the thymus[42,43]. However, Pdx1 has already been shown to be expressed in skin, linked to the development of papillomas in KC mice[44]. To finally confirm our hypothesis, it would be interesting to perform Pdx1 labelling on thymus and thymic masses, which will allow to discriminate between sporadic or Pdx1-induced recombination. However, Pdx1 expression in thymic cells would probably be transient, and could thus be difficult to highlight. In addition, sporadic recombination is favored by the presence of repeated sequences[45,46], as can be considered Lox sequences surrounding transcriptional STOP upstream *Kras*^{G12D} allele added by Jackson and colleagues in 2001[24], and lymphocyte population have been shown to be sensitive to Kras activation[47], encouraging the sporadic recombination hypothesis.

The KC mouse model is one of the most used models to study pancreatic carcinogenesis. We thus investigated the impact of thymic mass development on this process. Unfortunately, we highlighted that thymic tumor occurrence was associated with an accelerated pancreatic carcinogenesis. Indeed, these mice developed more pancreatic lesions and with higher grade. In addition, we detected some KRAS^{G12D}-positive cells within the adjacent spleen, suggesting an invasive phenotype for pancreatic (pre)tumoral cells. Thus, the presence of thymic tumor affects the study of the pancreatic carcinogenesis process. The accelerated carcinogenesis could be due to immune disorder within these mice. This hypothesis is corroborated by (1) the disorganization we observed within the spleen, with the perturbation of white pulp structure, and (2) high level of (immune) infiltration within the pancreas of one mouse with thymic mass. Indeed, disorder in thymus could affect T cell compartment and lead to the absence or the inefficiency of tumor-suppressing immune response in first steps of pancreatic carcinogenesis[48]. In addition, in the mouse presenting high level of immune infiltration, it was interesting to note that lymph nodes and immune cells around pancreatic cells were positive for KRAS^{G12D} protein, as well as in spleen white pulp, suggesting either (1) sporadic recombination or (2) the recruitment of immune cells from thymic mass.

Finally, the labelling of KRAS^{G12D} was also quite interesting to understand the appearance of lesions in pancreas of KC mice. Indeed, we detected KRAS^{G12D} within preneoplastic lesions, as well as in Langerhans islets, as expected by the expression of *Pdx1* in these structures[25,33,34]. The presence of KRAS^{G12D} in the islets could explain the islet disorganization, as well as the lesions developing within islets that have been previously described[35,36]. Interestingly, we also highlighted KRAS^{G12D} in acinar cells surrounding pre-tumoral lesions and evoking first steps of ADM (less contiguous acini and with more visible light), suggesting that *Pdx1* expression could be induced by the lesion and lead to transformation of adjacent normal acinar cells.

Our study thus pointed out an adverse effect of the *Kras*^{G12D} construct in the KC mouse model classically used to study pancreatic carcinogenesis. To our knowledge, this is the first report showing the development of such thymic tumors in the KC mouse model. The hypothesis of sporadic recombination in organs with high level of recombination (thymus notably) is favored here. This bias is associated with an accelerated pancreatic carcinogenesis, and can thus lead to misinterpretations, knowing that thymic mass can be missed if only the pancreas is recovered (without opening the rib cage).

Methods

Animals

LSL:*Kras*^{G12D} (B6.129S4-*Kras*^{tm4Tyj}/J strain, The Jackson Laboratory) and *Pdx1*-CRE (B6.FVB-Tg(Pdx1-cre)6Tuv/J strain, The Jackson Laboratory) mouse strains were previously described[24,25,41] and generously gifted by P. Bertolino and L. Bartholin, respectively. They were maintained in two pathogen-free animal facilities (''ALECS-SPF" and "PBES" (Lyon, France)), and crossed in order to obtain [LSL:*Kras*^{G12D};*Pdx1*-CRE] mice, predisposed to pancreatic cancer development. All procedures were conducted in accordance with the guidelines of the European Union and French laws and approved by the local animal ethic committee under regulatory of governmental authority (CECCAPP, Comité d'Evaluation Commun au Centre Léon Bérard, à l'Animalerie de transit de l'ENS, au PBES et au laboratoire P4 (n° C2EA15), APAFIS #16242-201804271428498). The study was carried out in compliance with the ARRIVE guidelines (Animal Research : Reporting of In Vivo Experiments)[49]. Animals were genotyped one week after birth and euthanized either at 100 or 150 days post-parturition or at reaching end-point (weight loss, signs of pain, *etc*). Several organs were harvested, including pancreas, spleen, lung, thymus, as well as the tail for control. After dissection, one part of each organ (except tail) was fixed in formalin before being processed for paraffin embedding. Other part was directly snap frozen in liquid nitrogen for DNA extraction.

Histological staining and immunohistochemistry

For histological analyses, formalin-fixed paraffin embedded (FFPE) tissues were cut into 3µm sections and Hematoxylin and Eosin (H&E) staining was performed after dewaxing and rehydration.

Immunohistochemistry staining on FFPE tissues was performed on 3µm sections using ImmPRESS® Excel Amplified Polymer Staining Kit, Anti-Rabbit IgG, Peroxidase (VectorLaboratories, MP-7601) for Ki67 and KRAS^{G12D}, and R.T.U. Vectastain Universal Elite ABC Kit (VectorLabs, PK-7200) for CK19, following manufacturer's instructions. After deparaffinization and rehydration, antigen retrieval was performed either in Sodium Citrate buffer (pH 6) for 20min at 98°C followed by 20min cooling (Ki67 and CK19) or 30min in pepsin reagent (Sigma, R2283) at 37°C (KRAS^{G12D}). Then, endogenous peroxidases were quenched and slices were saturated with 2.5% Horse Serum. Primary antibodies (CK19, 1/100, #TROMA-III-s (DHSB); Ki67, prediluted, #RMPD-004 (Clinisciences); KRAS^{G12D}, 1/50, #14429 (Cell Signaling)) were incubated in blocking solution or 1% Horse Serum (KRAS^{G12D}) overnight at 4°C. The next day, amplification and development were performed following manufacturer's instructions, nuclei were counterstained with Gill's Hematoxylin and slices were mounted in DEPEX. All slices were imaged using the slide scanner AxioScanSP5 X (Zeiss) at CIQLE (Lyon, France) in order to have a general view of all tissues. Representative images were then extracted and shown in this article.

Kras^{G12D} PCR

Genomic DNA extraction was performed by incubating tissues for 30min in alkaline lysis solution (25mM NaOH, 0.2mM Na_2EDTA) at 95°C. Tissue lysis was stopped by adding neutralization solution (40mM Tris-HCl) (v/v) on ice.

[LSL:*Kras*^{G12D};*Pdx1*-CRE] mice were genotyped by PCR amplification of genomic DNA from tail, as advised for this mouse strain (https://www.jax.org/Protocol?stockNumber=008179&protocolID=29388). PCR mix was composed of 1X TAQ polymerase buffer, 2.5mM MgCl2, 1mM dNTP (each), 1µM primers (each), 1U TAQ Polymerase. Primers used were: (p1) 5' TGTCTTTCCCCAGCAGAGT 3', (p2) 5' CTGCATAGTACGCTATACCCTGT 3', (p3) 5' GCAGGTCGAGGGACCTAATA 3'. 2 µl of DNA was added to the

mix and PCR was performed following cycles: 5min at 96°C, 35 cycles (30s at 96°C, 35s at 60°C, 45s at 72°C), 5min at 72°C. PCR amplicons were separated on a 2% (w/v) agarose gel in order to detect the 250bp wild-type *Kras* and 100bp floxed LSL:*Kras*^{G12D} products.

Kras^{G12D} conditional PCR was performed on thymus, pancreas and tail genomic DNA as mentioned by The Jackson laboratories (https://jacks-lab.mit.edu/protocols/genotyping/kras_cond). PCR mix was composed of 1X TAQ polymerase buffer, 2.5mM MgCl2, 0.4mM dNTP (each), 0.4µM primers (each), 1U TAQ Polymerase. Primers used were: (p1) 5' GTCTTTCCCCAGCACAGTGC 3', (p2) 5' CTCTTGCCTACGCCACCAGCTC 3', (p3) 5' AGCTAGCCACCATGGCTTGAGTAAGTCTGCA 3'. 1 µl of DNA was added to the mix and PCR was performed following cycles: 5min at 96°C, 35 cycles (30s at 96°C, 30s at 63°C, 45s at 72°C), 5min at 72°C. PCR amplicons were separated on a 2% (w/v) agarose gel in order to detect the 622bp wild-type *Kras,* 500bp floxed LSL:*Kras*^{G12D} and 650bp recombined *Kras*^{G12D} products. Position of primers and expected results are presented in Figure 1.

References

1. Ferlay, J. *et al.* Estimating the global cancer incidence and mortality in 2018: GLOBOCAN sources and methods. *International Journal of Cancer* **144**, 1941–1953 (2019).
2. Rahib, L. *et al.* Projecting Cancer Incidence and Deaths to 2030: The Unexpected Burden of Thyroid, Liver, and Pancreas Cancers in the United States. *Cancer Res* **74**, 2913–2921 (2014).
3. Quante, A. S. *et al.* Projections of cancer incidence and cancer-related deaths in Germany by 2020 and 2030. *Cancer Medicine* **5**, 2649–2656 (2016).
4. Rawla, P., Sunkara, T. & Gaduputi, V. Epidemiology of Pancreatic Cancer: Global Trends, Etiology and Risk Factors. *World J Oncol* **10**, 10–27 (2019).
5. Eibl, A. S. and G. Pancreatic Ductal Adenocarcinoma. *Pancreapedia: The Exocrine Pancreas Knowledge Base* (2015) doi:10.3998/panc.2015.14.
6. Walter, F. M. *et al.* Symptoms and patient factors associated with diagnostic intervals for pancreatic cancer (SYMPTOM pancreatic study): a prospective cohort study. *The Lancet Gastroenterology & Hepatology* **1**, 298–306 (2016).
7. Adamska, A., Domenichini, A. & Falasca, M. Pancreatic Ductal Adenocarcinoma: Current and Evolving Therapies. *Int J Mol Sci* **18**, (2017).
8. Behrens, D., Walther, W. & Fichtner, I. Pancreatic cancer models for translational research. *Pharmacology & Therapeutics* **173**, 146–158 (2017).
9. Krempley, B. D. & Yu, K. H. Preclinical models of pancreatic ductal adenocarcinoma. *Chinese Clinical Oncology* **6**, (2017).
10. Ding, Y., Cravero, J. D., Adrian, K. & Grippo, P. Modeling pancreatic cancer in vivo: from xenograft and carcinogen-induced systems to genetically engineered mice. *Pancreas* **39**, 283–292 (2010).
11. Bartholin, L. Pancreatic cancer and the tumor microenvironment: Mesenchyme's role in pancreatic carcinogenesis. in *Pancreatic Cancer and Tumor Microenvironment* (eds. Grippo, P. J. & Munshi, H. G.) (Transworld Research Network, 2012).
12. Ijichi, H. Genetically-engineered mouse models for pancreatic cancer: Advances and current limitations. *World Journal of Clinical Oncology* **2**, 195–202 (2011).
13. Pérez–Mancera, P. A., Guerra, C., Barbacid, M. & Tuveson, D. A. What We Have Learned About Pancreatic Cancer From Mouse Models. *Gastroenterology* **142**, 1079–1092 (2012).

14. Mazur, P. K. & Siveke, J. T. Genetically engineered mouse models of pancreatic cancer: unravelling tumour biology and progressing translational oncology. *Gut* **61**, 1488–1500 (2012).
15. Kong, K., Guo, M., Liu, Y. & Zheng, J. Progress in Animal Models of Pancreatic Ductal Adenocarcinoma. *J Cancer* **11**, 1555–1567 (2020).
16. Wagner, M. *et al.* A murine tumor progression model for pancreatic cancer recapitulating the genetic alterations of the human disease. *Genes Dev.* **15**, 286–293 (2001).
17. Sandgren, E. P., Luetteke, N. C., Palmiter, R. D., Brinster, R. L. & Lee, D. C. Overexpression of TGF alpha in transgenic mice: induction of epithelial hyperplasia, pancreatic metaplasia, and carcinoma of the breast. *Cell* **61**, 1121–1135 (1990).
18. Jančík, S., Drábek, J., Radzioch, D. & Hajdúch, M. Clinical Relevance of KRAS in Human Cancers. *Journal of Biomedicine and Biotechnology* vol. 2010 e150960 https://www.hindawi.com/journals/bmri/2010/150960/ (2010).
19. Weng, C.-C., Lin, Y.-C. & Cheng, K.-H. The Use of Genetically Engineered Mouse Models for Studying the Function of Mutated Driver Genes in Pancreatic Cancer. *J Clin Med* **8**, (2019).
20. Kattan, W. E. & Hancock, J. F. RAS Function in cancer cells: translating membrane biology and biochemistry into new therapeutics. *Biochemical Journal* **477**, 2893–2919 (2020).
21. Timar, J. & Kashofer, K. Molecular epidemiology and diagnostics of KRAS mutations in human cancer. *Cancer Metastasis Rev* **39**, 1029–1038 (2020).
22. Buscail, L., Bournet, B. & Cordelier, P. Role of oncogenic KRAS in the diagnosis, prognosis and treatment of pancreatic cancer. *Nat Rev Gastroenterol Hepatol* **17**, 153–168 (2020).
23. O'Hagan, R. C. & Heyer, J. KRAS Mouse Models. *Genes Cancer* **2**, 335–343 (2011).
24. Jackson, E. L. *et al.* Analysis of lung tumor initiation and progression using conditional expression of oncogenic K-ras. *Genes Dev.* **15**, 3243–3248 (2001).
25. Hingorani, S. R. *et al.* Preinvasive and invasive ductal pancreatic cancer and its early detection in the mouse. *Cancer Cell* **4**, 437–450 (2003).
26. Hingorani, S. R. *et al.* Trp53R172H and KrasG12D cooperate to promote chromosomal instability and widely metastatic pancreatic ductal adenocarcinoma in mice. *Cancer Cell* **7**, 469–483 (2005).
27. Aguirre, A. J. *et al.* Activated Kras and Ink4a/Arf deficiency cooperate to produce metastatic pancreatic ductal adenocarcinoma. *Genes Dev.* **17**, 3112–3126 (2003).
28. Guerra, C. & Barbacid, M. Genetically engineered mouse models of pancreatic adenocarcinoma. *Molecular Oncology* **7**, 232–247 (2013).
29. Ashizawa, S., Brunicardi, F. C. & Wang, X.-P. PDX-1 and the pancreas. *Pancreas* **28**, 109–120 (2004).
30. Vinogradova, T. V. & Sverdlov, E. D. PDX1: A unique pancreatic master regulator constantly changes its functions during embryonic development and progression of pancreatic cancer. *Biochemistry Moscow* **82**, 887–893 (2017).
31. Habbe, N. *et al.* Spontaneous induction of murine pancreatic intraepithelial neoplasia (mPanIN) by acinar cell targeting of oncogenic Kras in adult mice. *Proc Natl Acad Sci U S A* **105**, 18913–18918 (2008).
32. Tuveson, D. A. & Hingorani, S. R. Ductal Pancreatic Cancer in Humans and Mice. *Cold Spring Harb Symp Quant Biol* **70**, 65–72 (2005).
33. Park, J. Y. *et al.* Pdx1 Expression in Pancreatic Precursor Lesions and Neoplasms. *Appl Immunohistochem Mol Morphol* **19**, 444–449 (2011).

34. Tang, Z.-C., Chu, Y., Tan, Y.-Y., Li, J. & Gao, S. Pancreatic and duodenal homeobox-1 in pancreatic ductal adenocarcinoma and diabetes mellitus. *Chin Med J (Engl)* **133**, 344–350 (2020).
35. Gout, J. *et al.* The conditional expression of KRAS G12D in mouse pancreas induces disorganization of endocrine islets prior the onset of ductal pre-cancerous lesions. *Pancreatology* **13**, 191–195 (2013).
36. Friedlander, S. Y. G. *et al.* Context-Dependent Transformation of Adult Pancreatic Cells by Oncogenic K-Ras. *Cancer Cell* **16**, 379–389 (2009).
37. Hasserjian, R. P., Ströbel, P. & Marx, A. Pathology of thymic tumors. *Seminars in Thoracic and Cardiovascular Surgery* **17**, 2–11 (2005).
38. Pearse, G. Histopathology of the Thymus. *Toxicol Pathol* **34**, 515–547 (2006).
39. Huo, X. *et al.* Analysis of the relationship between microsatellite instability and thymic lymphoma induced by N-methyl-N-nitrosourea in C57BL/6J mice. *Mutation Research/Fundamental and Molecular Mechanisms of Mutagenesis* **771**, 21–28 (2015).
40. Dudgeon, C. *et al.* The evolution of thymic lymphomas in p53 knockout mice. *Genes Dev* **28**, 2613–2620 (2014).
41. Johnson, L. *et al.* Somatic activation of the K-ras oncogene causes early onset lung cancer in mice. *Nature* **410**, 1111–1116 (2001).
42. Noso, S. *et al.* Insulin Transactivator MafA Regulates Intrathymic Expression of Insulin and Affects Susceptibility to Type 1 Diabetes. *Diabetes* **59**, 2579–2587 (2010).
43. Brimnes, M. K. *et al.* Low Expression of Insulin in the Thymus of Non-obese Diabetic Mice. *Journal of Autoimmunity* **19**, 203–213 (2002).
44. Mazur, P. K. *et al.* Identification of Epidermal Pdx1 Expression Discloses Different Roles of Notch1 and Notch2 in Murine KrasG12D-Induced Skin Carcinogenesis In Vivo. *PLOS ONE* **5**, e13578 (2010).
45. Klein, H. L. Genetic control of intrachromosomal recombination. *BioEssays* **17**, 147–159 (1995).
46. Andersen, S. L., Sloan, R. S., Petes, T. D. & Jinks-Robertson, S. Genome-Destabilizing Effects Associated with Top1 Loss or Accumulation of Top1 Cleavage Complexes in Yeast. *PLOS Genetics* **11**, e1005098 (2015).
47. Kindler, T. *et al.* K-RasG12D–induced T-cell lymphoblastic lymphoma/leukemias harbor Notch1 mutations and are sensitive to γ-secretase inhibitors. *Blood* **112**, 3373–3382 (2008).
48. Vonderheide, R. H. & Bayne, L. J. Inflammatory networks and immune surveillance of pancreatic carcinoma. *Current Opinion in Immunology* **25**, 200–205 (2013).
49. Percie du Sert, N. *et al.* The ARRIVE guidelines 2.0: Updated guidelines for reporting animal research*. *J Cereb Blood Flow Metab* **40**, 1769–1777 (2020).

Acknowledgments

We greatly thank members of the histology and imaging facility (PrImaTiss) at the LBTI institute, as well as we acknowledge the contribution of Federative Structure of Health Research Lyon-Est CNRS UMS3453 / INSERM US7 and particularly the microscopy platform (CIQLE) and the specific pathogen-free animal facility (ALECS-SPF). Finally, we thank Dr. Philippe BERTOLINO and Dr. Laurent BARTHOLIN (Cancer Research Center of Lyon (CRCL), UMR INSERM 1052, UMR CNRS 5286) for providing us the $KRAS^{G12D}$-driven mouse model and Laurent GENESTIER (CRCL, INSERM U1052, UMR CNRS 5286) for its expert advice regarding thymic lymphoma in mouse models. SL is recipient of PhD student fellowship from the French government (NMRT). This work was supported by the "Ligue Nationale contre le Cancer, Comité du Rhône", "Comité de l'Allier", "Comité de Savoie" and "Comité de la Drôme", as well as by the "Fondation ARC pour la recherche sur le cancer" (PJA 20141201790).

Author contributions

S.L. and E.L. designed the experiments. S.L. and N.E.K. performed the experiments. S.L., N.E.K. and E.L. analyzed the experimental results. S.L. prepared all figures. S.L. wrote the main manuscript text. B.V. and U.V. acquired the financial support for the project. All authors were involved in critical reading of the paper prior to submission.

Competing Interests Statement

The authors declare no competing financial or non-financial interest in relation to the work described.

Figure Legends

Figure 1: KC (LSL:*$Kras^{G12D}$*:Pdx1-CRE;) mouse model. *(**a**) Schematic representation of the genetic construct for conditional* $Kras^{G12D}$ *expression under the control of* Pdx1 *promoter (CRE-Lox system). Primers used for* $Kras^{G12D}$ *conditional PCR are noticed. (**b**) Top:* $Kras^{G12D}$ *conditional PCR showing LSL cassette recombination in pancreas, but not tail, from KC mouse, and not in WT mouse. Bottom:* $Kras^{G12D}$ *genotyping PCR showing heterozygosity in KC mice (WT and* $Kras^{G12D}$ *alleles) and homozygosity in WT mouse (WT allele). Uncropped gels are provided in Supplementary Figure S3.*

Figure 2: 10% of KC mice exhibited rapid weight loss and decreased survival associated with thymic mass development. *(**a**) Weight tracking of 7 of the 8 KC mice presented in this study (3 without thymic mass (the* 4^{th} *having been euthanized before the start of weighing, at 100 days) and 4 with thymic mass revealed during dissection). (**b**) Cumulative survival proportion depending on the development (orange, n=4) or not (green, n=4) of thymic mass. (**c**) Photo of the rib cage at autopsy, showing normal thymus (left) and the thymic mass developed in 10% of KC mice (right). Dotted line delimits thymus.*

Figure 3: Thymic mass showed a lymphoma-like histology and total LSL cassette recombination associated with $KRAS^{G12D}$ ***expression in all cells.*** *(**a**) Representative images of normal thymus and thymic mass histologically analyzed (H&E staining and Ki67 immunohistochemistry). C = cortex, M = medulla. (**b**) Top:* $Kras^{G12D}$ *conditional PCR showing LSL cassette recombination in thymic mass but not in normal thymus and tail (KC mice). Bottom:* $Kras^{G12D}$ *genotyping PCR showing heterozygosity in all KC mice of this study (WT and* $Kras^{G12D}$ *alleles). Uncropped gels are provided in Supplementary Figure S3. (**c**) Representative images of* $KRAS^{G12D}$ *protein expression in normal thymus and thymic mass (immunohistochemistry).*

Figure 4: KC mice developing thymic tumor exhibited accelerated pancreatic carcinogenesis, immune perturbations and lung malignancies. *(**a**) Representative images of pancreas from KC mice showing or not thymic mass analyzed by classical histology (H&E staining) and immunohistochemistry (Ki67, CK19 and KRAS^{G12D}), and quantification of the area occupied by lesions in pancreas sections. (**b**) Representative images of histological analysis of spleen from KC mice presenting or not thymic mass (H&E staining and Ki67 and Kras^{G12D} immunohistochemistry). (**c**) Image showing enlarged spleen from KC mouse with thymic mass. (**d**) Representative images of histological analysis of lung from KC mice with or without thymic mass (H&E staining and Ki67, CK19 and Kras^{G12D} immunohistochemistry). Bottom: This mouse displayed moderate lesions in lung. (**e**) Picture showing severe lung lesions, macroscopically visible, from KC mouse presenting thymic mass at autopsy. (**a,b,d**) Arrowheads highlight KRAS^{G12D} staining.*

Figures

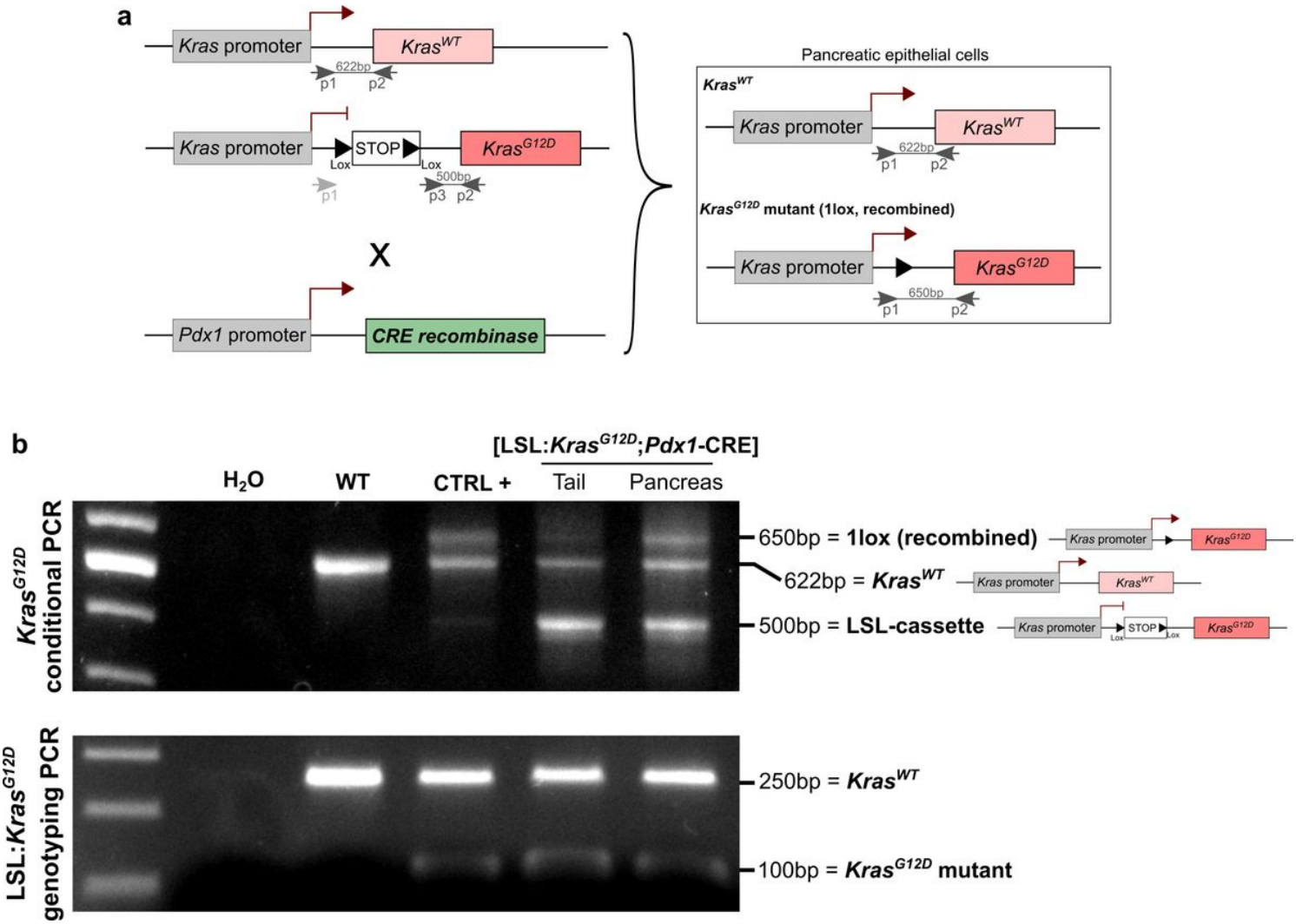

Figure 1

KC (LSL:KrasG12D:Pdx1-CRE;) mouse model. (a) Schematic representation of the genetic construct for conditional KrasG12D expression under the control of Pdx1 promoter (CRE-Lox system). Primers used for KrasG12D conditional PCR are noticed. (b) Top: KrasG12D conditional PCR showing LSL cassette recombination in pancreas, but not tail, from KC mouse, and not in WT mouse. Bottom: KrasG12D genotyping PCR showing heterozygosity in KC mice (WT and KrasG12D alleles) and homozygosity in WT mouse (WT allele). Uncropped gels are provided in Supplementary Figure S3.

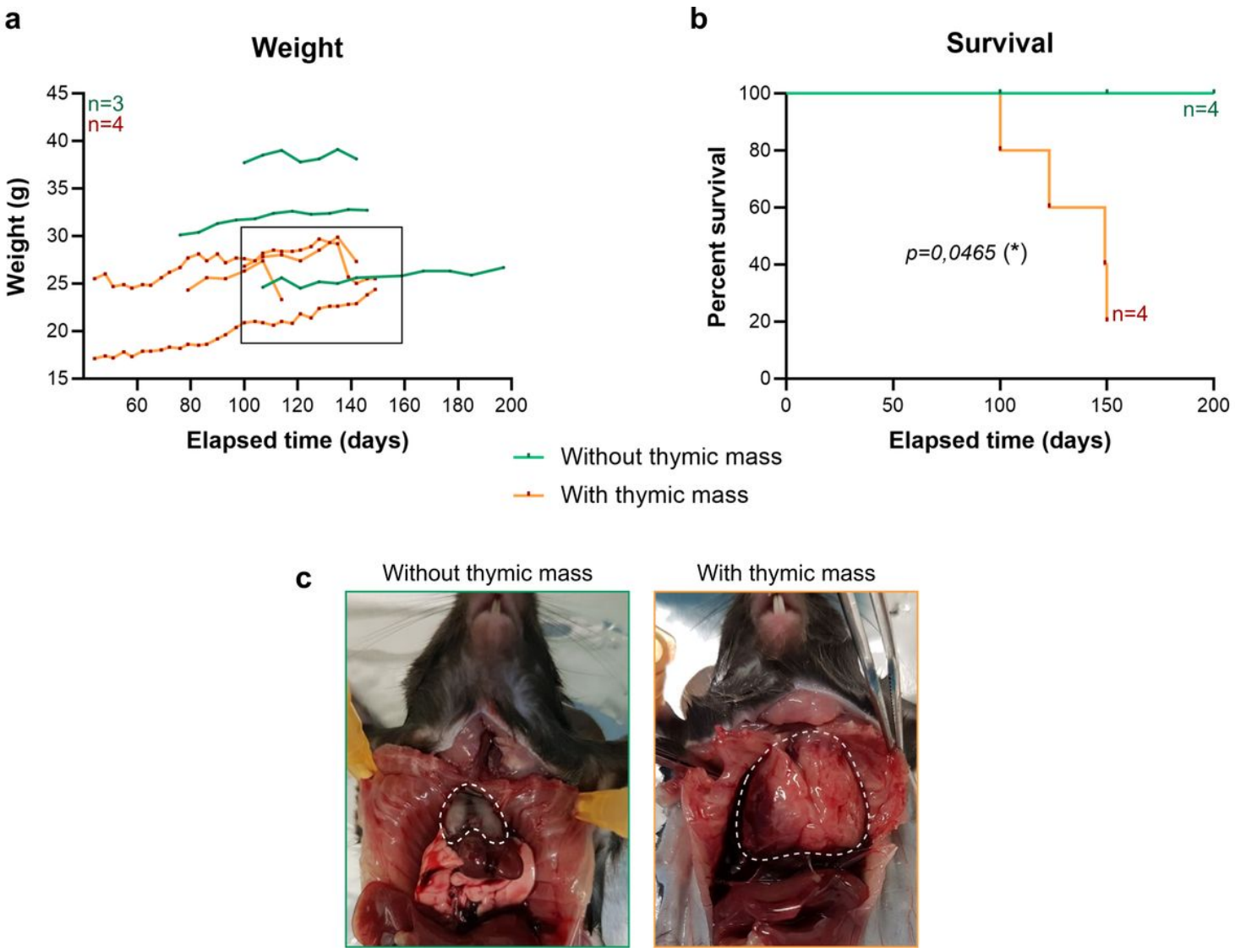

Figure 2

10% of KC mice exhibited rapid weight loss and decreased survival associated with thymic mass development. (a) Weight tracking of 7 of the 8 KC mice presented in this study (3 without thymic mass (the 4th having been euthanized before the start of weighing, at 100 days) and 4 with thymic mass revealed during dissection). (b) Cumulative survival proportion depending on the development (orange, n=4) or not (green, n=4) of thymic mass. (c) Photo of the rib cage at autopsy, showing normal thymus (left) and the thymic mass developed in 10% of KC mice (right). Dotted line delimits thymus.

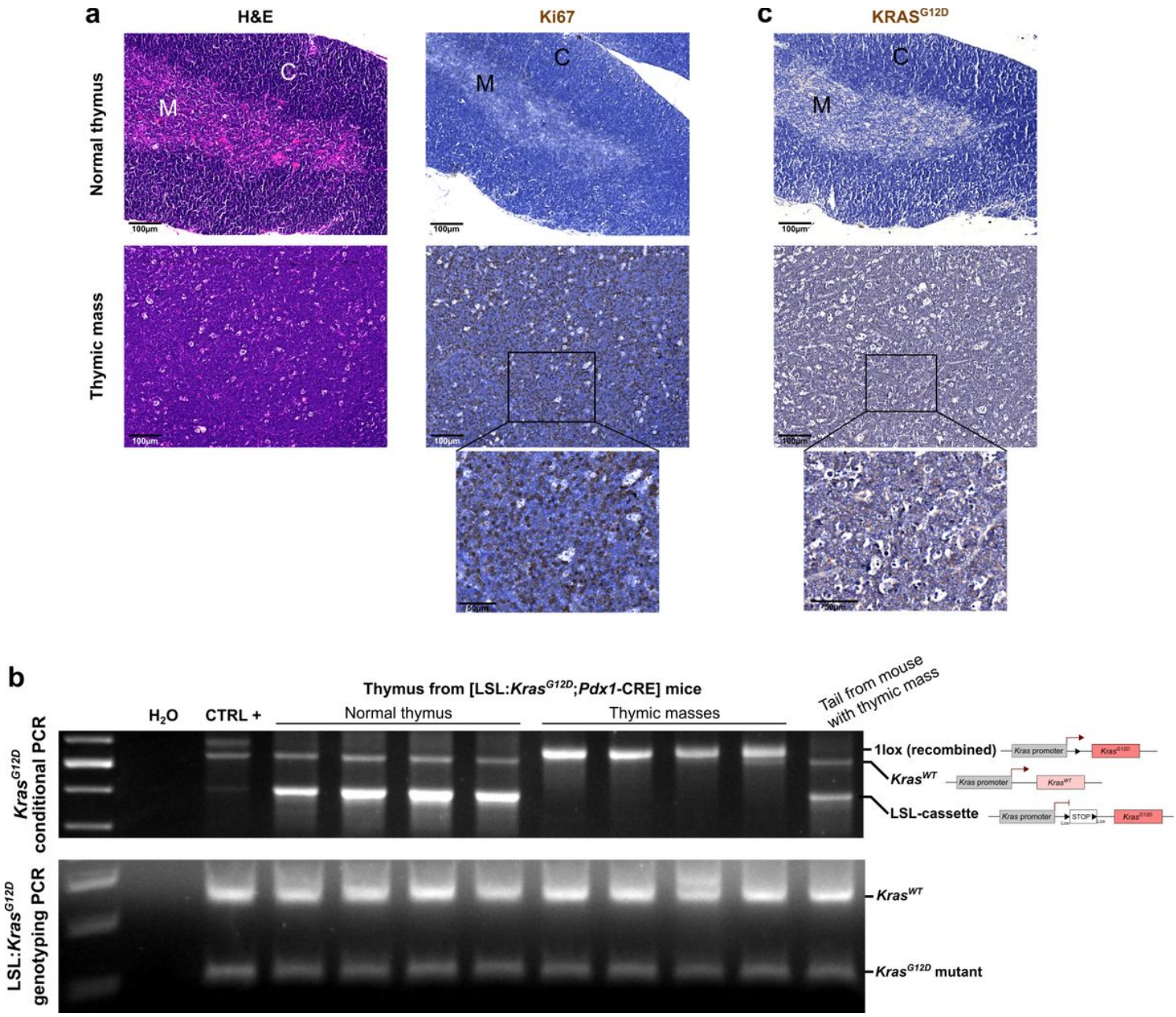

Figure 3

Thymic mass showed a lymphoma-like histology and total LSL cassette recombination associated with KRASG12D expression in all cells. (a) Representative images of normal thymus and thymic mass histologically analyzed (H&E staining and Ki67 immunohistochemistry). C = cortex, M = medulla. (b) Top: KrasG12D conditional PCR showing LSL cassette recombination in thymic mass but not in normal thymus and tail (KC mice). Bottom: KrasG12D genotyping PCR showing heterozygosity in all KC mice of this study (WT and KrasG12D alleles). Uncropped gels are provided in Supplementary Figure S3. (c) Representative images of KRASG12D protein expression in normal thymus and thymic mass (immunohistochemistry).

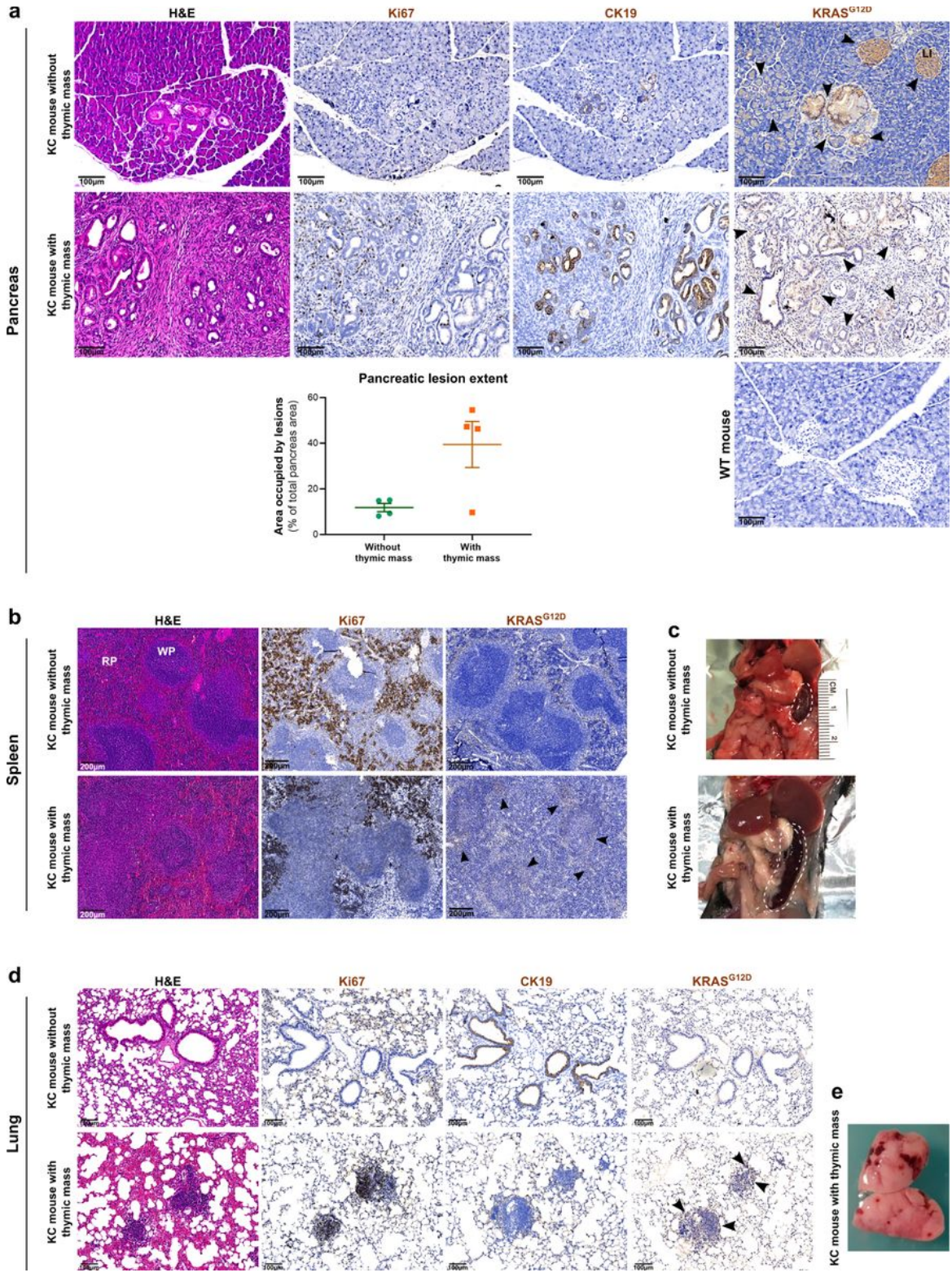

Figure 4

KC mice developing thymic tumor exhibited accelerated pancreatic carcinogenesis, immune perturbations and lung malignancies. (a) Representative images of pancreas from KC mice showing or not thymic mass analyzed by classical histology (H&E staining) and immunohistochemistry (Ki67, CK19 and KRASG12D), and quantification of the area occupied by lesions in pancreas sections. (b) Representative images of histological analysis of spleen from KC mice presenting or not thymic mass (H&E staining and

Ki67 and KrasG12D immunohistochemistry). (c) Image showing enlarged spleen from KC mouse with thymic mass. (d) Representative images of histological analysis of lung from KC mice with or without thymic mass (H&E staining and Ki67, CK19 and KrasG12D immunohistochemistry). Bottom: This mouse displayed moderate lesions in lung. (e) Picture showing severe lung lesions, macroscopically visible, from KC mouse presenting thymic mass at autopsy. (a,b,d) Arrowheads highlight KRASG12D staining.

Supplementary Files

This is a list of supplementary files associated with this preprint. Click to download.

- SupplementaryFiguresv2.pdf